Foot and Ankle Surgery 25 (2019) 371–377

Contents lists available at ScienceDirect

Foot and Ankle Surgery

journal homepage: www.elsevier.com/locate/fas

The geometrical axis of the talocrural joint—Suggestions for a new measurement of the talocrural joint axis

Leif Claassen[a,*,1], Philipp Luedtke[a,1], Daiwei Yao[a], Sarah Ettinger[a], Kiriakos Daniilidis[b], Andrej M. Nowakowski[c], Magdalena Mueller-Gerbl[d], Christina Stukenborg-Colsman[a], Christian Plaass[a]

[a] Orthopedic Department of the Hannover Medical School at DIAKOVERE Annastift, Germany
[b] Sporthopaedicum Straubing, Straubing, Germany
[c] Orthopedic Department, University Hospital Basel, Switzerland
[d] Institute of Anatomy, University of Basel, Switzerland

ARTICLE INFO

Article history:
Received 6 November 2017
Received in revised form 4 January 2018
Accepted 2 February 2018

Keywords:
Ankle joint
Talocrural joint
Total ankle replacement
Joint axis
CT-scan

ABSTRACT

Background: Despite intensive research there is no consensus about the talocrural joint axis. The aim of the present study is a new method to determinate the geometric rotational axis of the talocrural joint.
Methods: We analyzed 98 CT-scans of full cadaver Caucasian legs. We generated three-dimensional reconstruction models of the talus. A best fitting cone was orientated to the talar articular surface. The geometric rotational axis was defined to be the axis of this cone.
Results: The geometric rotational axis of the talocrural joint is orientated from lateral–distal to medial–proximal (85.6° ± 10 compared to anatomical tibial axis in torsional plane), from posterior–distal to anterior–proximal (81.43° ± 44.35 compared to anatomical tibial axis in sagittal plane) and from posterior–medial to anterior–lateral (169.2° ± 5.91 compared to intermalleolar axis in axial plane).
Conclusions: The consideration of our results might be helpful for better understanding of ankle biomechanics.

© 2018 European Foot and Ankle Society. Published by Elsevier Ltd. All rights reserved.

1. Introduction

A thorough knowledge of anatomy and biomechanics of joints is crucial for implant design and positioning. Mal-positioning has been shown to be one cause for implant failure [1]. Further on, the correct placement of the implant may improve function and reduce pain after joint replacement in patients.

In modern knee and hip arthroplasty kinematic alignment orientated on the joint axis gained more consideration to improve the clinical results and reduce the rate of postoperative disorders and the revision rate [2]. Especially for the knee joint recent patient-specific implantation techniques tried to consider the rotational axis and positioned the implants orientated to this axis [2,3]. To restore the physiologic joint function the preoperative determination of joint axis, planning of implant position and a high intraoperative accuracy of implant placement is necessary.

Ankle arthritis is a limiting and painful disease with an increasing incidence. In severe cases the preferred treatment options are arthrodesis or total ankle replacement (TAR) [4]. Until now the arthrodesis is predominantly used compared to TAR [5]. With the development of improved implants, the number of performed TAR rose within the last decades [6,7]. Nevertheless, the revision rate after TAR remained between 10% and 39% [7,8], which is high compared to revision rates after total knee or hip replacement [9,10]. Beside the different etiologies of arthritis in the ankle compared to the other joints, reasons for persistent disorders and higher revision rate might be an insufficient consideration of the anatomy, biomechanics and the limited predictability due to use of conventional radiographs for planning of the prothesis, all potential leading to a malalignment of the prosthesis [11,12].

The biomechanics of the ankle joint and the complex relationship to the hindfoot mobility is less understood than in many other joints. Still there is no consensus about the rotational axis of the talocrural joint [13–18].

* Corresponding author at: Hannover Medical School, Orthopedic Department, Anna-von-Borries-Stra 1-7, Hannover 30625, Germany.
E-mail addresses: leif.claassen@diakovere.de (L. Claassen), philipp.luedtke@stud.mh-hannover.de (P. Luedtke), daiwei.yao@diakovere.de (D. Yao), sarah.ettinger@diakovere.de (S. Ettinger), kraj@gmx.de (K. Daniilidis), andrej.nowakowski@usb.ch (A.M. Nowakowski), m.mueller-gerbl@unibas.ch (M. Mueller-Gerbl), christina.stukenborg@diakovere.de (C. Stukenborg-Colsman), christian.plaass@diakovere.de (C. Plaass).
[1] Shared first authorship.

https://doi.org/10.1016/j.fas.2018.02.003
1268-7731/© 2018 European Foot and Ankle Society. Published by Elsevier Ltd. All rights reserved.

The aim of the present study was to evaluate a new method of geometrically determining the TJA of the ankle.

2. Material and methods

2.1. Cadaver

We analyzed 98 computer tomography (CT) scans of Caucasian full cadaver legs. The age of the patients averaged 81 (range: 44–104) years, 50 legs were from female patients, 48 from male patients. There were no signs of previous trauma, severe deformity or degenerative changes in the legs. All legs were eligible for analysis and the anatomical structures could be identified. All cadavers were fixed by perfusion via the femoral artery using a solution containing 8500 ml ethanol, 750 ml 37% aqueous formalin solution, 250 ml 2-phenoxyethanol, and 250 ml glycerin. Consecutively the cadavers had been fixed by immersion in ethanol solution for at least 1 year. CT scans were performed in supine position using the Siemens Emotion 16 (2007), with an X-ray tube current of 126 mA, KVP 130 kV. The slice thickness was 1.5 mm in joint areas of hip, knee and ankle.

2.2. Coordinate system and segmentation

Initially, all scans were imported into the software Mimics® (Version 20.0, Materialise©, Leuven, Belgium). The data sets were resliced in accordance to the following coordinate system: the torsional plane is containing the tips of the medial (MM) and lateral malleolus (LM) and the inter-condylar point (IC) located midway between the most medial and most lateral points of the tibial condyles. The sagittal plane is perpendicular to the torsional plane containing the IC and the inter-malleolar point (IM) located midway between MM and LM. The axial plane is perpendicular to torsional and sagittal plane. The center of the coordinate system is the IM. Hence, the y-axis connects IM and IC. The x axis is perpendicular to the sagittal plane and the z-axis perpendicular to the torsional plane. (Fig. 1).

These chosen reference points are in accordance with the recommendations by the International Society of Biomechanics (ISB) and were used in previous studies [16,17,19–21]. Moreover, the anatomic tibial axis (ATA) was defined as the line between the anatomical center of the proximal and the distal tibial plateau. The inter-malleolar axis (IMA) was defined as a line connecting MM and LM.

After reslicing, geometric models of talus and tibia with fibula were segmented automatically via thresholding (Hounsfield unit = 226-3071). Then 3-D-models of the segmented bones were created via Mimics® (Materialise©, Leuven, Belgium).

The used coordinate system based on the ISB recommendations is illustrated (MM = most inferior point of the medial malleolus; LM = most inferior point of the lateral malleolus; IM = the midpoint of the line connecting MM and LM; MC = most medial point of the border of the medial tibial condyle; LC = most lateral point of the border of the lateral tibial condyle; IC = the midpoint of the line connecting MC and LC) [21]

2.3. Geometric rotational axis

GOM inspect software (Version 8.0, Gesellschaft für optische Messtechnik©, Braunschweig, Germany) enables to create a best fitting cone to any surface. We applied this tool to the talar articular surface of segmented tali (Figs. 2 and 3). The talar articular surface was defined as the area between the transition from convexity and concavity from talus dome to talus neck anteriorly and to the processus posterior tali posteriorly. The mediolateral borders were defined by the shoulders of the talus dome. The reliability of this method was determined by an independent evaluation by three

Fig. 1. Coordinate system.

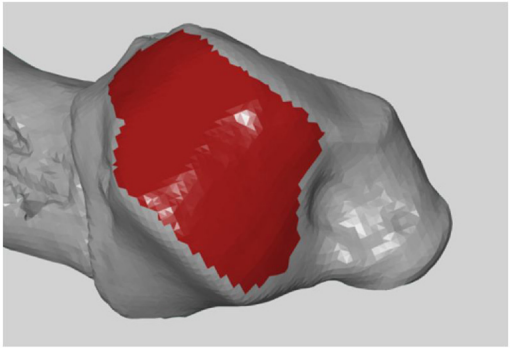

Fig. 2. Marked joint surface.
The best fitting cone that connects all marked points (827 points ± 286) is applied.

foot and ankle surgeons three times each for ten tali and in repetition four weeks later. The cone was optimized resulting in the least possible deviation. The axis of the cone was defined to be the geometric talar joint axis (GTJA) (Fig. 4).

The GTJA was transferred into Mimics® and the angles between the GTJA and the anatomic tibial axis (ATA) in torsional and sagittal plane were evaluated (Fig. 5). In addition, the angle between the IMA and the GTJA was determined in the axial plane (Fig. 5). Moreover, the

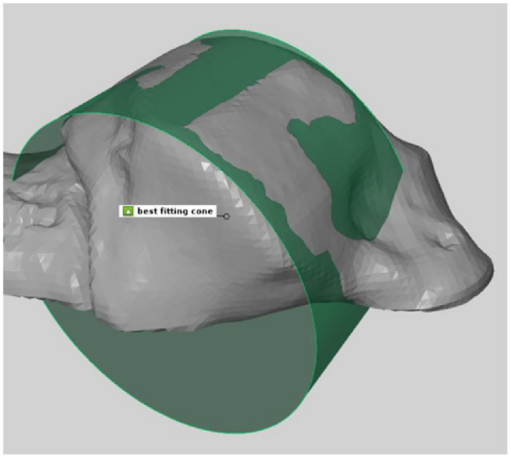

Fig. 3. Best fitting cone.
The cone is applied to the articular surface of the talus.

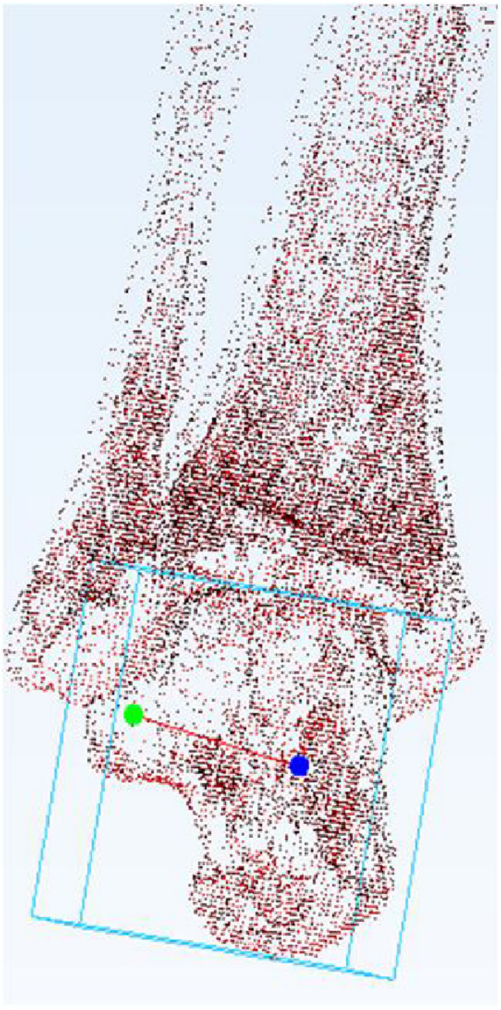

Fig. 4. Geometric talocrural joint axis.
The axis of the cone was deemed to be the GTJA. We determined the angles of the joint axis to the torsional, sagittal and axial plane.

angles between the GTJA and the defined planes themselves (torsional, sagittal, axial) were evaluated via 3-matic® (Version 10.0, Materialise©, Leuven, Belgium) (Fig. 6). All measurements were compared between male and female legs and depending on the age in statistical analyses. Regarding the comparison of the GTJA the angle was measured proximal/medial in torsional plane, proximal/anterior in sagittal plane and medial/anterior in axial plane.

2.4. Statistical analysis

The statistical analysis was performed with IBM SPSS Statistics© (Version 24.0, IBM©, Armonk, New York 10504). We used a two-sided unpaired Student's t-test for data on interval scale. Additionally we used the interclass correlation coefficient (ICC) for assessment of the inter- and intrarater reliability. The values are expressed as mean with standard deviation, p-values with $p < 0.05$ being significant.

3. Results

3.1. Reliability of the best fitting cone determination

The reliability of the best fitting cone was established using an intraclass coefficient of correlation (ICC) analysis. The reliability of the procedure was determined by multiple repetition of three different surgeons and the same surgeon giving an ICC of 0.87 for interrater correlation and an ICC of 0.92 for intrarater correlation. These ICCs were considered high for the current purposes. The average number of points for each cone was 827.3 ± 286.2. The average maximum distance of the furthest point to the talar articular surface was $0.41\ mm \pm 0.09$.

3.2. Geometric rotational axis

In comparison to the ATA the GTJA is orientated from lateral–distal to medial–proximal (torsional plane), from posterior–distal to anterior–proximal (sagittal plane). Moreover, it is orientated from medial–posterior to lateral–anterior in comparison to the IMA (axial plane). Noteworthy we found a high variability especially for the sagittal plane. This orientation is additionally illustrated in comparison to the standardized planes. (Table 1 and Figs. 7 and 8).

4. Discussion

Although the TJA is a fundamental component of the biomechanics of the ankle it is still a subject of discussion. Not only its orientation is contentious, but also whether there is only one axis or multiple axes (Table 2). With the present study we present a new and reproducible method to detect GTJA via 3D-models based on CT scans.

In the present study we used full leg CT scans. In contrast to other studies analyzing only the talus or the foot with the distal tibia we were able to compare the GTJA against the ATA. CT scans were widely used in previous studies and give detailed information about bony anatomy and assures measurement in a physiologic range [29–32]. This seems to be reasonable as the cartilage layer of the ankle joint is very homogenous and thin with a mean cartilage thickness of the talar articular surface of 1.1 mm and of the tibial articular surface of 1.16 mm [33]. CT scans are not as susceptible as plain radiographs to ankle position and rotation of the shank [34,35]. Additionally, CT-scans are to prefer compared to MRI datasets as they are cheaper and easier to evaluate due to higher resolution. Our coordinate system was based on ISB recommendations. Thereby we applied a standardized and validated system as used by several authors [16,17,19,36]. For segmentation and analyses we used the established products of Materialise© likewise to previous authors [17,37–39]. This enables to resclice the CT scans regarding to the coordinate system, generate 3D-models and provides the analyze tools needed for the present study. Additionally we used GOM inspect, a software

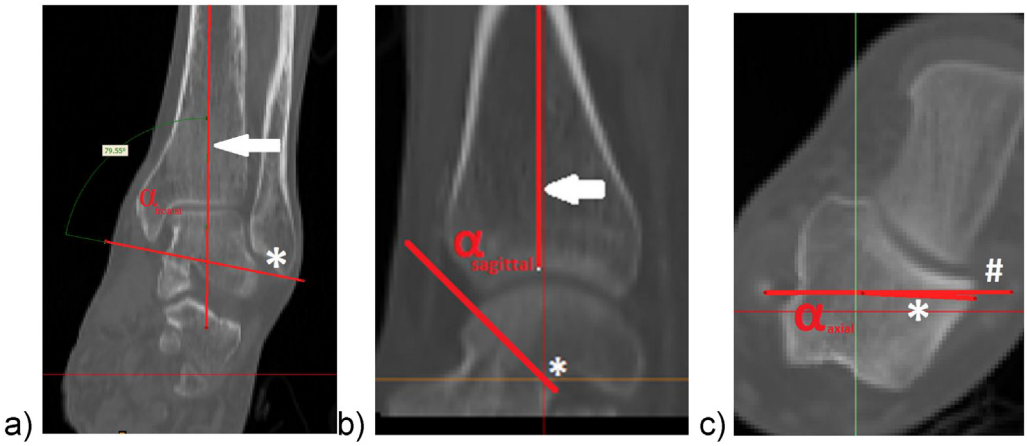

Fig. 5. Geometric talocrural joint axis vs. anatomic tibial axis in torsional and sagittal plane or vs. intermalleolar axis in axial plane.
The assessment is illustrated for the torsional plane (a), the sagittal plane (b) and the axial plane (c); star = GTJA, arrow = ATA, pound = IMA.

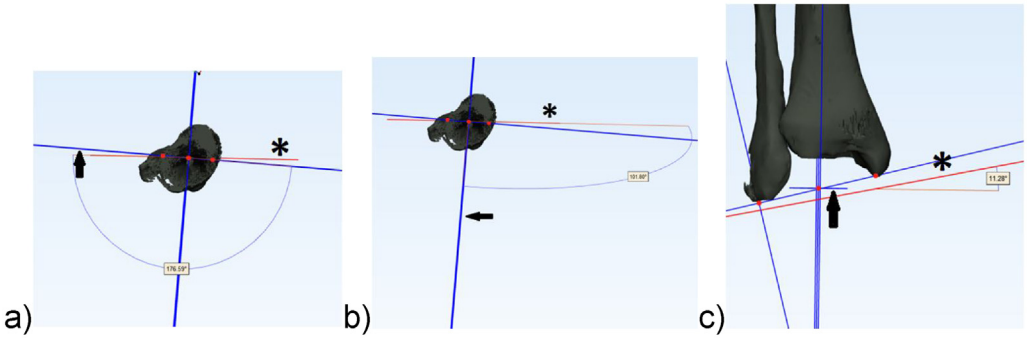

Fig. 6. Geometric talocrural joint axis vs. defined planes.
The angles of the GTJA against the torsional plane (a), sagittal plane (b) and the axial plane (c); star = GTJA, arrow = the respective plane were determined.

Table 1
Geometric talocrural joint axis.

	All (n = 98)		Male (n = 48)		Female (n = 50)		p-Value
	Mean	SD	Mean	SD	Mean	SD	
GTJA to torsional plane	169.16	7.10	168.43	8.81	169.86	4.93	0.32
GTJA to sagittal plane	104.50	6.51	105.21	8.2	103.81	4.27	0.29
GTJA to axial plane	3.78	8.13	3.25	8.63	4.30	7.68	0.53
GTJA-ATA in torsional plane	85.60	9.98	86.38	10.22	84.86	9.79	0.45
GTJA-ATA in sagittal plane	81.43	44.35	78.99	45.63	83.78	43.42	0.60
GTJA-IMA in axial plane	169.20	5.91	168.67	6.73	169.7	5.01	0.39
	All (n = 98)		< 80 (n = 36)		≥80 (n = 62)		p-Value
	Mean	SD	Mean	SD	Mean	SD	
GTJA to torsional plane	169.16	7.10	167.03	8.76	170.39	5.65	0.02
GTJA to sagittal plane	104.50	6.51	105.07	8.48	104.17	5.07	0.51
GTJA to axial plane	3.78	8.13	2.73	6.66	4.40	8.87	0.33
GTJA-ATA in torsional plane	85.60	9.98	87.13	8.55	84.72	10.69	0.25
GTJA-ATA in sagittal plane	81.43	44.35	74.98	30.58	85.18	50.52	0.27
GTJA-IMA in axial plane	169.20	5.91	167.56	5.68	170.15	5.87	0.04

The results of the evaluation of the GTJA are illustrated. There were relevant differences for the orientation of the TJA to the torsional plane and in the axial plane regarding the age ($p = 0.02$ and $p = 0.04$). There were no significant differences for gender ($p > 0.05$).

for applying a best fitting cone as used by previous authors [40,41]. Furthermore the cone was directly based on the talar articular surface without any further manual step. However, the selection of the articular surface area might be a base for a system immanent error. This possible error was little as low inter- and intrarater deviations showed. The transfer of the axis from GOM inspect to the Materialise© products was done digitally. Likewise the software performed the comparison of the GTJA against the defined planes without any further possibility for system immanent errors. In contrast the comparison of GTJA against the ATA or IMA was performed manually resulting in a higher risk for measurement errors.

Joint axes have been described in different forms. In the knee a multiple-axis model has been postulated [42,43], but later research

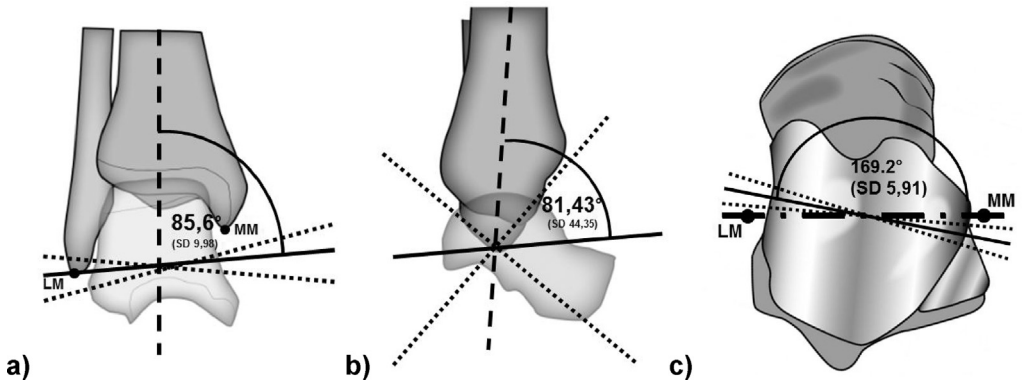

Fig. 7. GTJA in comparison to ATA and IMA.
The angles of the GTJA illustrated in the torsional plane (a), sagittal plane (b) and the axial plane (c); continuous line = GTJA, long dashed line = ATA, short dashed line = SD axis, short-long dashed line = IMA. Additionally MM and LM are illustrated.

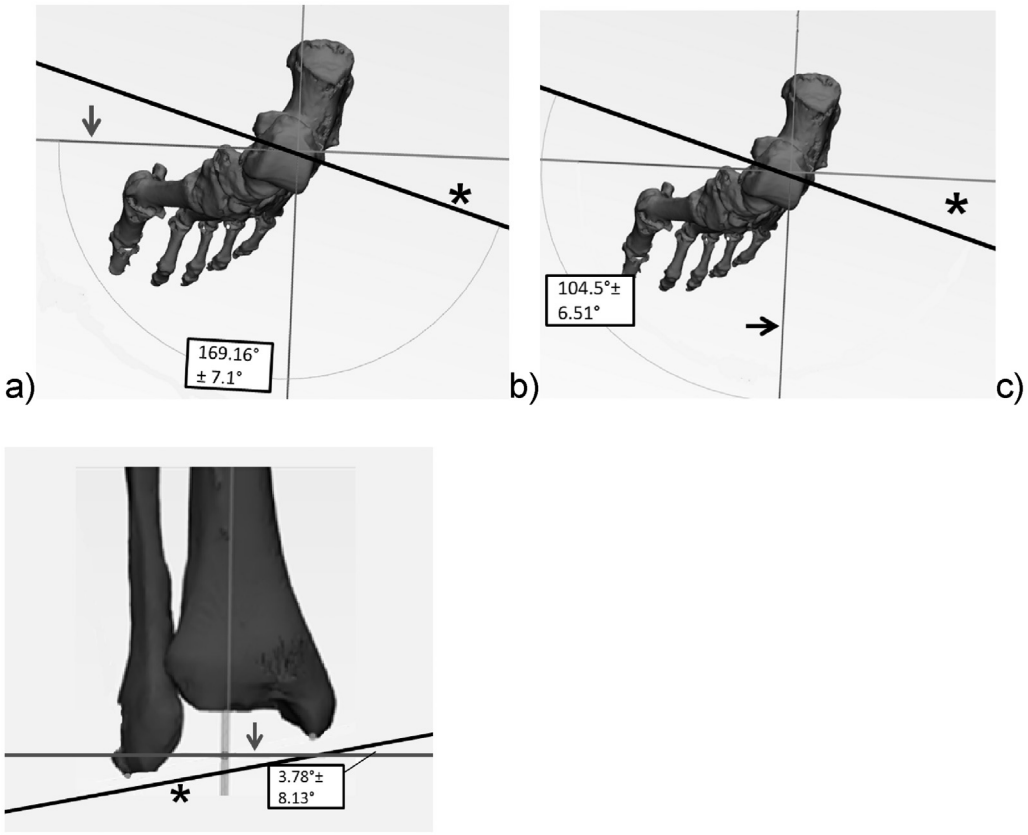

Fig. 8. GTJA in comparison to the defined planes.
The angles of the GTJA against the torsional plane (a), sagittal plane (b) and the axial plane (c) are marked.

showed, that its movement can better be described and reproduced by a single-axis model [44].

With our approach we generate a single-axis model of the ankle, which corresponds with the geometric form of the talus and is supported by the high congruency of the joint and the isometric stabilization. Nevertheless, several studies supported the theory, that a multiple joint axes model can describe the TJA. The main argument was a different radius of the anterior and the posterior talar articular surfaces. Thereby different axes depending on the position of the foot in dorsiflexion or plantarflexion were hypothesized [13,22,23,27,45,46]. On the other hand there are studies supporting a single axis model of the TJA. This applies especially for the physiological range of motion of the talocrural joint whereas a divergent joint axis beyond the physiological range of motion was not excluded [14–18]. Hence we cannot prove that our axis is the real biochemical axis of the talocrural joint. However, in accordance to the present study most publications described a distinct variability of the orientation of the TJA [13,15]

The proximal–medial angle compared to the ATA was 85.6° ± 9.98°. That is comparable to 82.7° ± 3.6° detected by Inman, 84.5° ± 13.9° by Sheehan and 84.4° ± 3.9° by Cho [16–18]. Our results for the sagittal plane are characterized by a high variability. One reason might be that the respective detected GTJA are oriented approximately end-on to the sagittal plane. Therefore small changes of the GTJA lead to large deviations. We detected a mean angle of 81.43° ± 44.35° compared to the anatomical tibial axis.

Table 2
Summary of previous studies on the talocrural joint axis of the talus and anatomical parameters of the foot.

Author, date	n	Method	Coordinate system	Orientation	Axis
Barnett and Napier [13]	152	Cadaver, static, NWB	n.n.	PF: dist. med. DF: dist. lat.	M
Lapidus [14]	n. n.	Cadaver, static, NWB	n.n.	n.n.	S
Inman [18]	49	Cadaver, static, NWB (max PF – DF)	n.n.	Dist. lat.	S
Lundberg et al. [22]	8	X-ray, in vivo, WB (PF – DF 30°-0-30°)	Coordinate system related to MM and LM	PF: dist. med DF: dist. lat	M
Van den Bogert et al. [23]	14	Cameras, test movements, in vivo, NWB (PF – DF)	x-axis: coincides with TJA, z-axis: runs through closest point on subtalar joint axis Center: closest point to subtalar joint axis	Dist. lat. posterior	S
Leardini et al. [24]	7	Stereophotogrammetry, in vivo, WB (PF – DF)	y-axis between IM and tibial tuberosity, frontal plane connects MM, LM and the head of the fibula	n.n	M
Seiler [25]	22	X-ray, cadaver, static, NWB	n.n.	Dist. lat. posterior	S
Parr et al. [20]	58	Surface laser scanner, cadaver, static, NWB	ISB	n.n.	S
Arndt et al. [15]	3	Cameras, gait analysis, in vivo, WB (PF – DF 9°-0-9°)	n.n.	Dist. lat. posterior	M
Siegler et al. [19]	15	MRI, movements in vivo (n = 7) and in vitro (n = 8), NWB and WB (neutral – inv)	ISB	n.n.	n.n.
De Asla et al. [26]	5	Fluoroscope, test movements (NWB) and gait analysis (WB) (max PF – DF)	Axial plane contains both apices of trochlea tali, sagittal plane is lowest fitting arc of the trochlea tali	n.n.	M
Imai et al. [27]	10	CT, in vivo, NWB (max PF – DF)	y-axis parallel to a line connecting center of heel and second metatarsal, z-axis along tibial shaft through ankle center	n.n.	n.n.
Sheehan [16]	25	MRI, Simulated toe-raise, in vivo, NWB (1–5° less than max PF – DF)	y-axis is parallel to the anterior aspect of the tibia in sagittal image, z-axis connects most medial and lateral points of tibia in sagittal image, center is the midpoint between points of z-axis	Dist. lat. posterior	S
Kuo et al. [28]	58	CT, cadaver, static, NWB	x-axis from calcaneal insertion of achillles tendon to head of second metatarsal, y-axis perpendicular to base plate, Center is geometric center of the talus	n.n.	n.n.
Cho et al. [17]	61	CT, cadaver, static, NWB	ISB and principle axis according to Beimers et al. and Parr et al.	Dist. lat. posterior	S

WB = weight bearing, NWB = non weight bearing, PF = plantarflexion, DF = dorsiflexion, inv = inversion, S = single axis, M = multiple axis.

Measurement of the TJA in the sagittal plane is characterized by large standard deviations in the literature as well. Translated to our system van den Bogert et al. evaluated an angle of 83.16°, Arndt et al. an angle of 56.4–82.5° and Sheehan an angle of 78° (SD = 41.7] as they measured the angle to a line perpendicular to the ATA [15,16,23]. For the axial orientation of the talocrural joint it is oriented from posterior–medial to anterior–lateral, compared to the IMA. We measured the angle between TJA and IMA. We measured an angle of 169.2° ± 5.91°. Van den Bogert et al. measured an angle of 161.9°. Sheehan measured an angle of 150.8° ± 12.2° translated to our system, as an axis rotated approximately 45° to the IMA was used [16] Our results are comparable to Parr and Cho comparing the axis orientation in their results as they used a similar coordinate system. However, they did not measure the angle in the axial image.

We deem the high variability of the orientation of the geometrical talocrural joint axis noteworthy. Likewise earlier studies found high interindividual differences [23,31]. Moreover, osteoarthritic ankles undergo structural changes, leading to individual composition of bone and ligaments [32]. The consideration of our results might be helpful for better understanding of ankle biomechanics.

The present study has the following limitations. The proposed method is not verified via biomechanic testings. Using CT scans there are the basic disadvantages of accessibility and the risk of radiation. Furthermore we are not able to provide information about dynamic changes of the TJA. Additionally, significant substance defects of the talar articular surface will affect the determination of the talocrural joint axis using the proposed method described in the present study. However, as we used a best fitting cone small defects will not have a relevant effect. Computer based algorithm might in the future be able to reconstruct the initial anatomy of the joint before arthritic changes became relevant. A similar procedure is performed in TKA, where the original cartilage thickness is calculated to optimize the fit of the prosthesis. Momentary yet to be defined deformations might make this method not applicable in some patients.

5. Conclusion

The study demonstrates the feasibility of a system for estimating the GTJA in relation to the talar articular surface based on 3D-models derived from CT-Scans. It shows a new reproducible model to analyze the axis of the talocrural joint and might further improve the understanding of the ankle joint. Noteworthy were high interindividual variations of the orientation of the talocrural joint. Whereas the results of the present study have to be validated in biomechanic testings they could contribute to the development and placement of total ankle arthroplasties.

Conflict of interest statement

The present study was supported by an investigator initiated research grant from Implantcast GmbH (Buxtehude, Germany).

References

[1] Espinosa N, Walti M, Favre P, Snedeker JG. Misalignment of total ankle components can induce high joint contact pressures. J Bone Jt Surg Am 2010;92A(May (5)):1179–87.

[2] Calliess T, Bauer K, Stukenborg-Colsman C, Windhagen H, Budde S, Ettinger M. PSI kinematic versus non-PSI mechanical alignment in total knee arthroplasty: a prospective, randomized study. Knee Surg Sports Traumatol Arthrosc 2017;25(June (6)):1743–8.
[3] Kotela A, Kotela I. Patient-specific computed tomography based instrumentation in total knee arthroplasty: a prospective randomized controlled study. Int Orthop 2014;38(10):2099–107.
[4] Raikin SM, Rasouli MR, Espandar R, Maltenfort MG. Trends in treatment of advanced ankle arthropathy by total ankle replacement or ankle fusion. Foot Ankle Int 2014;35(3):216–24.
[5] Kostuj T, Preis M, Walther M, Aghayev E, Krummenauer F, Röder C. German total ankle replacement register of the German Foot and ankle society (D.A.F.)—presentation of design and reliability of the data as well as first results. Z Orthop Unfall 2014;152(5):446–54.
[6] Terrell RD, Montgomery SR, Pannell WC, Sandlin MI, Inoue H, Wang JC, et al. Comparison of practice patterns in total ankle replacement and ankle fusion in the United States. Foot Ankle Int 2013;34(November (11)):1486–92.
[7] LaMothe J, Seaworth CM, Do HT, Kunas GC, Ellis SJ. Analysis of total ankle arthroplasty survival in the United States using multiple state databases. Foot Ankle Spec 2016;9(August (4)):336–41.
[8] Jastifer JR, Coughlin MJ. Long-term follow-up of mobile bearing total ankle arthroplasty in the United States. Foot Ankle Int 2015;36(February (2)):143–50.
[9] Dyrhovden GS, Fenstad AM, Furnes O, Gothesen O. Survivorship and relative risk of revision in computer-navigated versus conventional total knee replacement at 8-year follow-up. Actaorthopaedica 2016;(October):1–8.
[10] Singh J, Politis A, Loucks L, Hedden DR, Bohm ER. Trends in revision hip and knee arthroplasty observations after implementation of a regional joint replacement registry. Can J Surg 2016;59(October (5)):304–10.
[11] Klaue K, Zwipp H, Mittlmeier T, Espinosa N. Internal circular arc osteosynthesis of tibiotalocalcaneal arthrodesis. Unfallchirurg 2016;119(October (10)):885–9.
[12] Hintermann B, Barg A, Knupp M. Revision arthroplasty of the ankle joint. Orthopade 2011;40(November (11)):1000–7.
[13] Barnett CH, Napier JR. The axis of rotation at the ankle joint in man; its influence upon the form of the talus and the mobility of the fibula. J Anat 1952;86(1):1–9.
[14] Lapidus PW. Kinesiology and mechanical anatomy of the tarsal joints. Clin Orthop 1963;30:20–36.
[15] Arndt A, Westblad P, Winson I, Hashimoto T, Lundberg A. Ankle and subtalar kinematics measured with intracortical pins during the stance phase of walking. Foot Ankle Int 2004;25(May (5)):357–64.
[16] Sheehan FT. The instantaneous helical axis of the subtalar and talocrural joints: a non-invasive in vivo dynamic study. J Foot Ankle Res 2010;13(July (3)):13.
[17] Cho H-, Kwak D-, Kim I-. Analysis of movement axes of the ankle and subtalar joints: relationship with the articular surfaces of the talus. Proc Inst Mech Eng H J Eng Med 2014;228(10):1053–8.
[18] Inman VT. Inman's joints of the ankle. Williams & Wilkins: Baltimore, MD; 1976.
[19] Siegler S, Udupa JK, Ringleb SI, Imhauser CW, Hirsch BE, Odhner D, et al. Mechanics of the ankle and subtalar joints revealed through a 3D quasi-static stress MRI technique. J Biomech 2005;38(3):567–78.
[20] Parr WCH, Chatterjee HJ, Soligo C. Calculating the axes of rotation for the subtalar and talocrural joints using 3D bone reconstructions. J Biomech 2012;45(6):1103–7.
[21] Wu G, Siegler S, Allard P, Kirtley C, Leardini A, Rosenbaum D, et al. ISB recommendation on definitions of joint coordinate system of various joints for the reporting of human joint motion—part 1: ankle, hip, and spine. J Biomech 2002;35(April (4)):543–8.
[22] Lundberg A, Svensson OK, Nemeth G, Selvik G. The axis of rotation of the ankle joint. J Bone Jt Surg B 1989;71(1):94–9.
[23] van den Bogert AJ, Smith GD, Nigg BM. In vivo determination of the anatomical axes of the ankle joint complex: an optimization approach. J Biomech 1994;27(12):1477–88.
[24] Leardini A, O'Connor JJ, Catani F, Giannini S. A geometric model of the human ankle joint. J Biomech 1999;32(June (6)):585–91.
[25] Seiler H. Biomechanics and functional anatomy of the upper ankle. Orthopade 1999;28(6):460–8.
[26] de Asla RJ, Wan L, Rubash HE, Li G. Six DOF in vivo kinematics of the ankle joint complex: application of a combined dual-orthogonal fluoroscopic and magnetic resonance imaging technique. J Orthop Res 2006;24(May (5)):1019–27.
[27] Imai K, Tokunaga D, Takatori R, Ikoma K, Maki M, Ohkawa H, et al. In vivo three-dimensional analysis of hindfoot kinematics. Foot Ankle Int 2009;30(11):1094–100.
[28] Kuo C-, Lu H-, Leardini A, Lu T-, Kuo M-, Hsu H-. Three-dimensional computer graphics-based ankle morphometry with computerized tomography for total ankle replacement design and positioning. Clin Anat 2014;27(4):659–68.
[29] Hayes A, Tochigi Y, Saltzman C. Ankle morphometry on 3D-CT images. Iowa Orthop J 2006;26:1–4.
[30] Mauch F, Drews B. Magnetic resonance imaging and computed tomography. What is important in orthopedics and traumatology. Unfallchirurg 2016;119(October (10)):790–802.
[31] Lepojarvi S, Niinimaki J, Pakarinen H, Koskela L, Leskela H. Rotational dynamics of the talus in a normal tibiotalar joint as shown by weight-bearing computed tomography. J Bone Jt Surg Am 2016;98(April (7)):568–75.
[32] Wiewiorski M, Hoechel S, Anderson AE, Nowakowski AM, DeOrio JK, Easley ME, et al. Computed tomographic evaluation of joint geometry in patients with end-stage ankle osteoarthritis. Foot Ankle Int 2016;37(June (6)):644–51.
[33] Millington SA, Grabner M, Mag RW, Anderson DD, Hurwitz SR, Crandall JR. Quantification of ankle articular cartilage topography and thickness using a high resolution stereophotography system. Osteoarthr Cartil 2007;15(February (2)):205–11.
[34] Barg A, Amendola RL, Henninger HB, Kapron AL, Saltzman CL, Anderson AE. Influence of ankle position and radiographic projection angle on measurement of supramalleolar alignment on the anteroposterior and hindfoot alignment views. Foot Ankle Int 2015;36(November (11)):1352–61.
[35] McCann H, Stanitski D, Barfield W, Leupold J. The effect of tibial rotation on varus deformity measurement. J Pediatr Orthop 2006;26(May–June (3)):380–4.
[36] Sancisi N, Parenti-Castelli V, Corazza F, Leardini A. Helical axis calculation based on Burmester theory: experimental comparison with traditional techniques for human tibiotalar joint motion. Med Biol Eng Comput 2009;47(November (11)):1207–17.
[37] Saveh AH, Katouzian HR, Chizari M. Measurement of an intact knee kinematics using gait and fluoroscopic analysis. Knee Surg Sports Traumatol Arthrosc 2011;19(February (2)):267–72.
[38] Ochia RS, Inoue N, Renner SM, Lorenz EP, Lim T, Andersson GBJ, et al. Three-dimensional in vivo measurement of lumbar spine segmental motion. Spine 2006;31(August (18)):2073–8.
[39] Rawal BR, Ribeiro R, Malhotra R, Bhatnagar N. Anthropometric measurements to design best-fit femoral stem for the Indian population. Indian J Orthop 2012;46(January–February (1)):46–53.
[40] Szymor P, Kozakiewicz M, Olszewski R. Accuracy of open-source software segmentation and paper-based printed three-dimensional models. J Cranio MaxilloFac Surg 2016;44(February (2)):202–9.
[41] Ranusa M, Gallo J, Hobza M, Vrbka M, Necas D, Hartl M. Wear and roughness of bearing surface in retrieved polyethylene Bicon-Plus cups. Acta Chir Orthop Traumatol Cech 2017;84(June (3)):159–67.
[42] Kurosawa H, Walker P, Abe S, Garg A, Hunter T. Geometry and motion of the knee for implant and orthotic design. J Biomech 1985;18(7):487–91.
[43] Blacharski P, Somerset J, Murray D. 3-dimensional study of kinematics of human knee. J Biomech 1975;8(6):375–6.
[44] Hollister A, Jatana S, Singh A, Sullivan W, Lupichuk A. The axes of rotation of the knee. Clin Orthop 1993;290(May (290)):259–68.
[45] Siegler S, Chen J, Schneck CD. The three-dimensional kinematics and flexibility characteristics of the human ankle and subtalar joints—part I: kinematics. J Biomech Eng 1988;110(4):364–73.
[46] Siegler S, Toy J, Seale D, Pedowitz D. The Clinical Biomechanics Award 2013—presented by the International Society of Biomechanics: new observations on the morphology of the talar dome and its relationship to ankle kinematics. Clin Biomech 2014;29(1):1–6.